Supporting Information

for

Surface motif sensitivity of dual emissive gold nanoclusters for robust ratiometric intracellular imaging

Xuefen Lou,[‡a] Fanfan Yu,[‡a] Zheng Cao,[a] Yue Xu,[a] Lina Yang*[a] and Honglin Liu*[a,b]

[a] School of Food and Biological Engineering, Engineering Research Center of Bio-process, Ministry of Education, Hefei University of Technology, Hefei 230009, China

[b] State Key Laboratory of High Performance Ceramics and Superfine Microstructure, Shanghai, China

*Correspondence: liuhonglin@mail.ustc.edu.cn (H.L.) yangln@mail.ustc.edu.cn (L.Y.)

Experimental Section

Preparation of d-Au NCs.

The d-Au NCs were prepared by reacting of single emissive GSH-protected Au NCs (s-Au NCs) with 11-mercaptoundecanoic acid (11-MUA). First, s-Au NCs were synthesized as follows. Freshly prepared aqueous solution of $HAuCl_4$ (250 mM, 160 μl) and GSH (12 mM, 5 ml) were mixed with 14.84 ml of ultrapure water under gentle stirring of ~500 rpm at 25 ºC. The reaction solution was heated to 140 ºC under ~500 rpm of stirring for 1.5 h. 610 nm-emitted s-Au NCs with orange emission under UV light were formed. Then, d-Au NCs were prepared based on the s-Au NCs. Typically, 1 ml of s-Au NCs aqueous solution was mixed with 200 μL PBS (pH=9) solution, then 200 μL of 100 mM 11-MUA dissolved in ethanol was added into the solution. NaOH (0.5 M) was added to the mixture to bring pH to ~12. The mixed solution was allowed to react at room temperature for 40 h under stirring of 700 ~rpm. Finally, d-Au NCs with two PL peaks at 420 nm and 630 nm were obtained, showing strong pink emission under UV light.

Detection of Valine and Cr^{3+} by d-Au NCs.

The as-synthesized d-Au NCs were used to detecting valine and Cr^{3+}, respectively. Before detection, HCl (0.5 M) was first added into d-Au NCs aqueous solution to bring pH to ~9. For detection of valine, valine solutions with different concentrations (0-140 μM) were separately added into the d-Au NCs solution. The selectivity toward valine was evaluated by adding 150 μM of various kinds of amino acids instead of valine. For detection of Cr^{3+}, Cr^{3+} solutions with different concentrations (0-300 μM) were separately added into the d-Au NCs solution. The selectivity toward Cr^{3+} was evaluated by adding 300 μM of various kinds of metal ions instead of Cr^{3+}.

Intracellular assays.

The cytotoxicity of d-Au NCs was evaluated by Standard MTT assays. In brief, HeLa cells were incubated in 5% CO_2 for 24 h at 37 °C in 96-well assay plates. Then different concentrations (0, 50, 100, 150, 200, 250 μg/mL) of d-Au NCs were added. After incubating for another 24 h, the cells were washed three times by PBS buffer solution and then treated with 20 μL of 5 mg/ml MTT for additional 4 h incubation at 37 °C. Finally, DMSO (150 μL) was added to dissolve the formed precipitate. The absorbance values at 490 nm was

determined on the Microplate Reader and then the cell viability was estimated. For intracellular imaging, HeLa cells were cultured in Dulbecco's modified Eagle's medium (DMEM) containing 12% fetal bovine serum, 100 units/ml penicillin, and 100 units/ml streptomycin for 12 h with 5% CO_2 at 37 °C. Then, 100 μg/ml d-Au NCs were added into the Hela cells with incubation for 12 h. For bioimaging valine, the cells were washed for three times by PBS solution, followed by the addition of different concentrations (90, 200 μM) of valine for 1 h incubation. Similarly, for imaging Cr^{3+}, the d-Au NCs-treated cells were washed for three times by PBS solution, followed by the addition of different concentrations (150, 300 μM) of Cr^{3+} for 1 h incubation.

Verification experiment instructions for confirming that the d-Au NCs are novel synthesized product.

To further confirm that the d-Au NC product is not a simple mixture of s-Au NCs with blue emissive species, we separated the 11-MUA-protected Au NCs intermediate at 1 h with a single PL peak at 420 nm. Obviously, the single PL peak of either the s-Au NCs (Fig. S5, ESI†) or the 11-MUA-protected Au NC intermediate (Fig. S6b, ESI†) has completely different excitation dependent PL behavior from that of the d-Au NCs (Fig. S2c, ESI†). Then, we mixed the s-Au NCs and the 11-MUA–Au NCs intermediate together (Fig. S7, ESI†). The PL spectrum has no dual emission and the PL peak at 610 nm is not redshifted to 630 nm. Moreover, the mixture has no characteristic UV-vis absorption peak due to inhomogeneity, which is completely different from that of the d-Au NCs with two typical absorption peaks. Hence, d-Au NCs are a new type of NC with two PL peaks ascribed to the LMCT effect from two different surface motifs (Au(I)–11-MUA and Au(I)–GSH) to the Au(0) core, respectively.

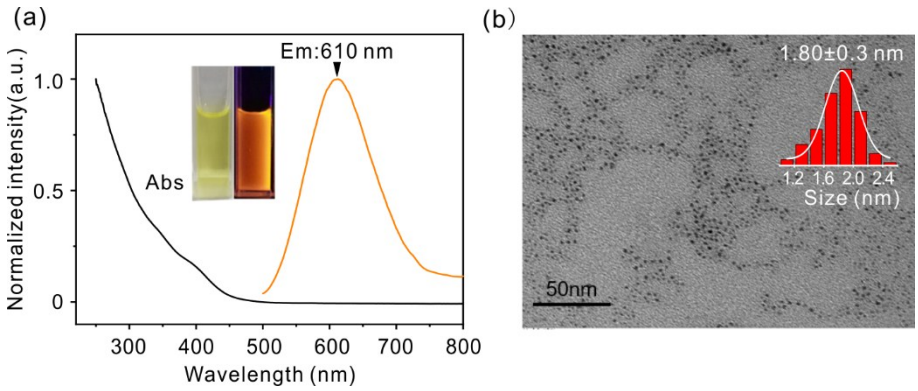

Figure S1. (a) PL and UV-vis absorption spectra of s-Au NCs. (Inset) The s-Au NCs solution under visible (left) and UV light (right). (b) TEM image of s-Au NCs.

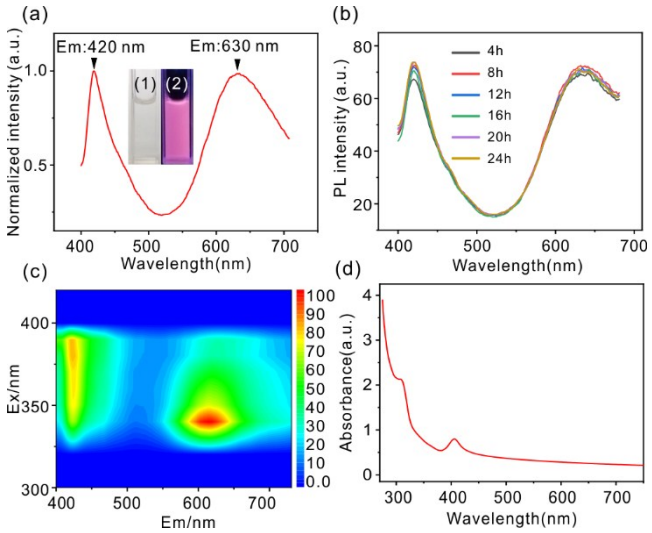

Figure S2. (a) PL spectrum of d-Au NCs (λ_{ex}=350 nm). (Insets) Digital photographs of d-Au NCs aqueous solutions under (1) visible and (2) UV light. (b) PL spectra of d-Au NCs after storage for different times. (c) PL excitation-emission mapping of d-Au NCs. (d) UV-vis absorption spectrum of d-Au NCs.

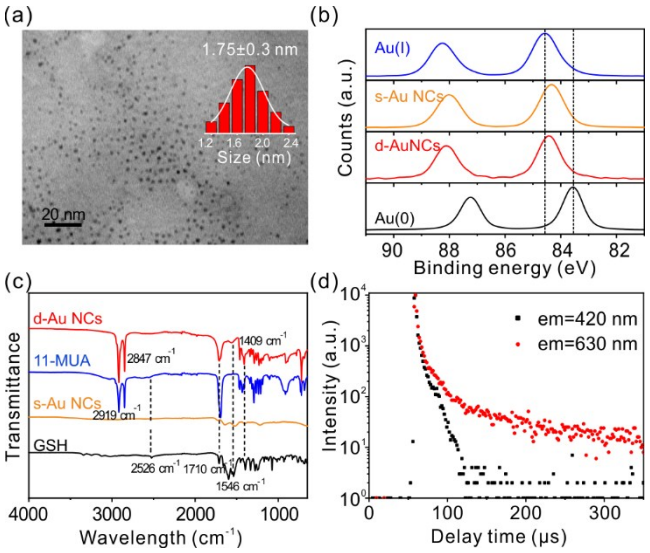

Figure S3. (a) TEM image of d-Au NCs. (b) Au 4f XPS spectra of Au(I)-thiolate complex (blue line), s-Au NCs (orange line), d-Au NCs (red line) and Au(0) nanocrystals (black line). (c) FTIR spectra of d-Au NCs (red line), 11-MUA (blue line), s-Au NCs (orange line) and GSH (black line). (d) Lifetimes of the two emission peaks at 420 and 630 nm.

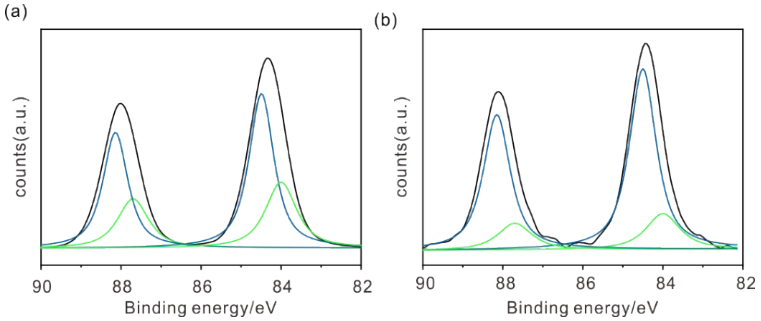

Figure S4. XPS spectra of s-Au NCs (a) and d-Au NCs (b) with deconvolution results. Raw spectra (black line), deconvolution of $4f_{7/2}$ and $4f_{5/2}$ bands into Au(0) (green line) and Au(I) (blue line).

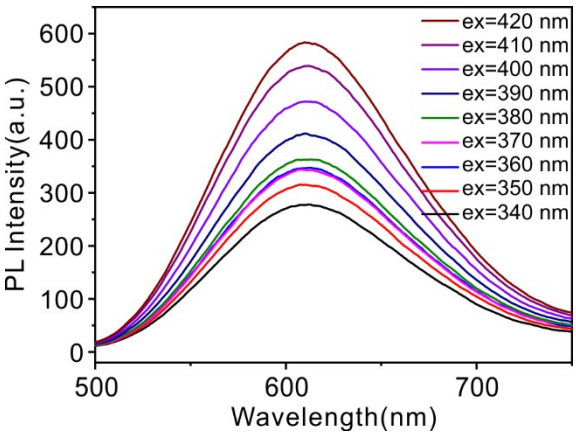

Figure S5. PL spectra of s-Au NCs under different excitation wavelengths

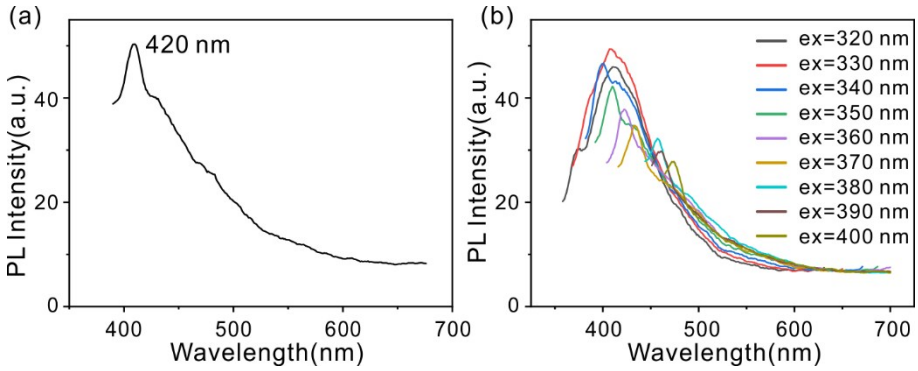

Figure S6. (a) PL spectrum of the blue emissive intermediate product at 1h with an emission peak at 420 nm (λ_{ex}=350 nm) (11-MUA-Au NCs intermediate). (b) PL spectra of the 11-MUA-Au NCs intermediate under different excitation wavelengths.

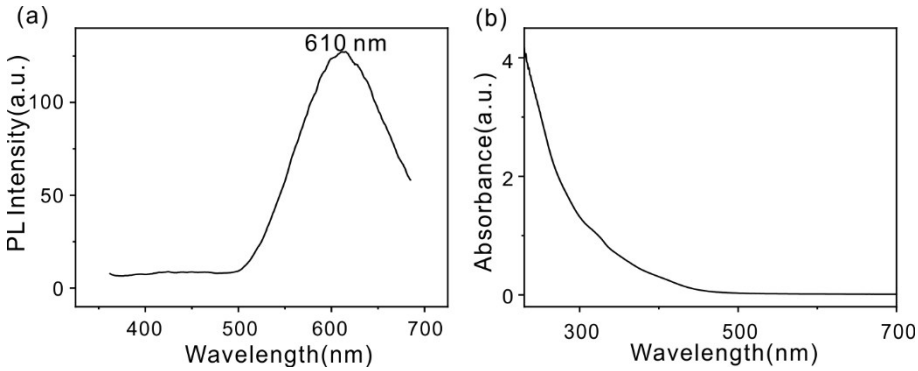

Figure S7. (a) PL and (b) UV-vis absorption spectrum of the direct mixture of s-Au NCs and 11-MUA-Au NCs intermediate.

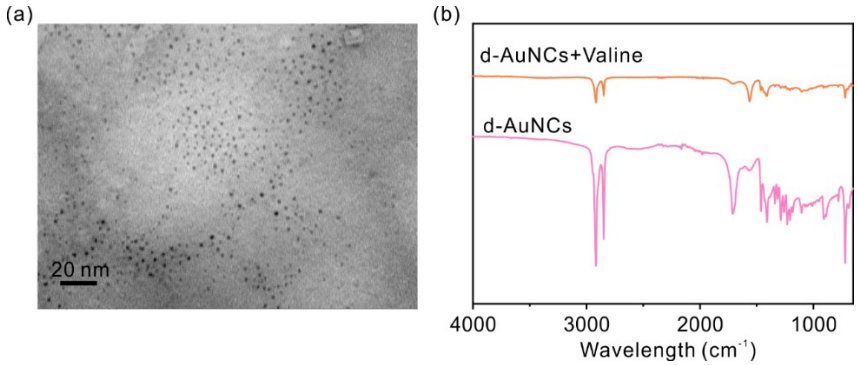

Figure S8. (a) TEM image of d-Au NCs after adding 140 μM of valine. (b) FT-IR spectra of d-Au NCs before and after adding 140 μM of valine.

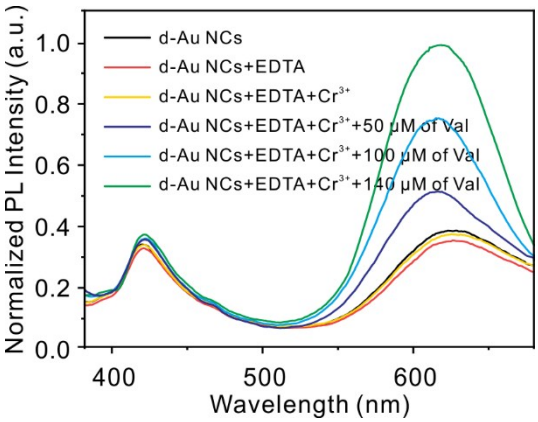

Figure S9. Experimental verification for eliminating Cr^{3+} interference by adding EDTA in detection of valine. PL spectra of d-Au NCs, d-Au NCs with adding 100 μM of EDTA, d-Au NCs with adding 100 μM of EDTA and 200 μM of Cr^{3+}, d-Au NCs with adding 100 μM of EDTA, 200 μM of Cr^{3+} and different concentrations of valine (50, 100, 140 μM).

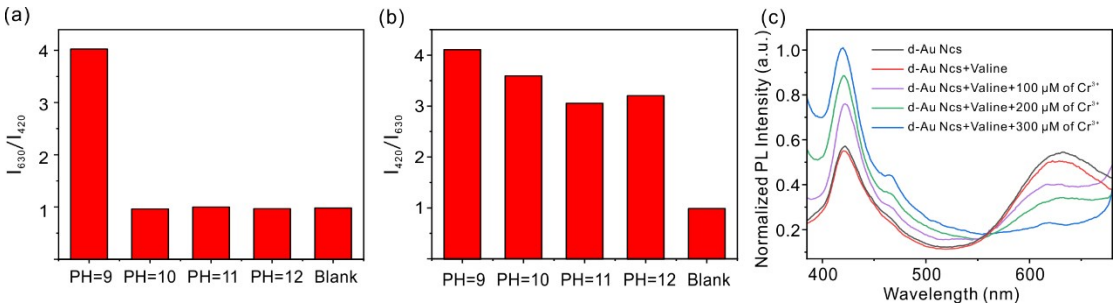

Figure S10. Experimental verification for eliminating valine interference by adjusting testing condition at pH 10.0 in detection of Cr^{3+}. (a) I_{630}/I_{420} values of d-Au NCs with 100 μM of valine under different pH. (b) I_{420}/I_{630} values of d-Au NCs with 200 μM of Cr^{3+} under different pH. (c) PL spectra measured under pH 10.0 for d-Au NCs, d-Au NCs with adding 100 μM of valine, d-Au NCs with adding 100 μM of valine and different concentrations (100, 200, 300 μM) of Cr^{3+}.

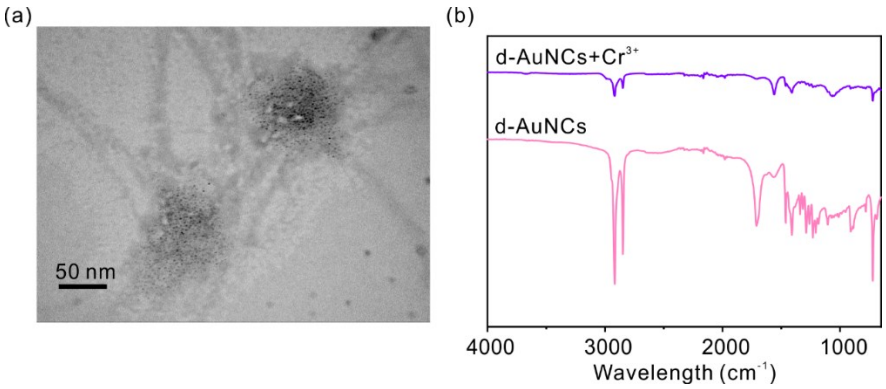

Figure S11. (a) TEM image of d-Au NCs after adding 300 μM of Cr^{3+}. (b) FT-IR spectra of d-Au NCs before and after adding 300 μM of Cr^{3+}.

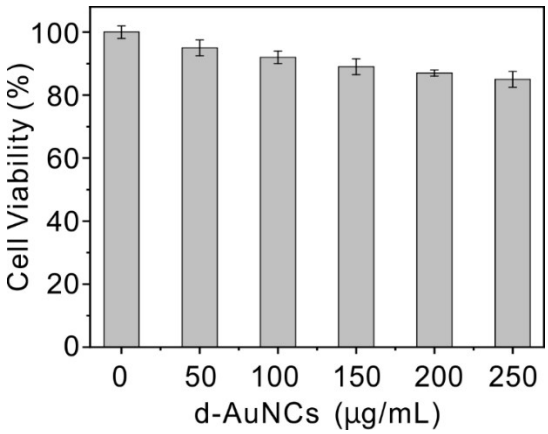

Figure S12. Cytotoxicity of d-Au NCs with different concentrations.

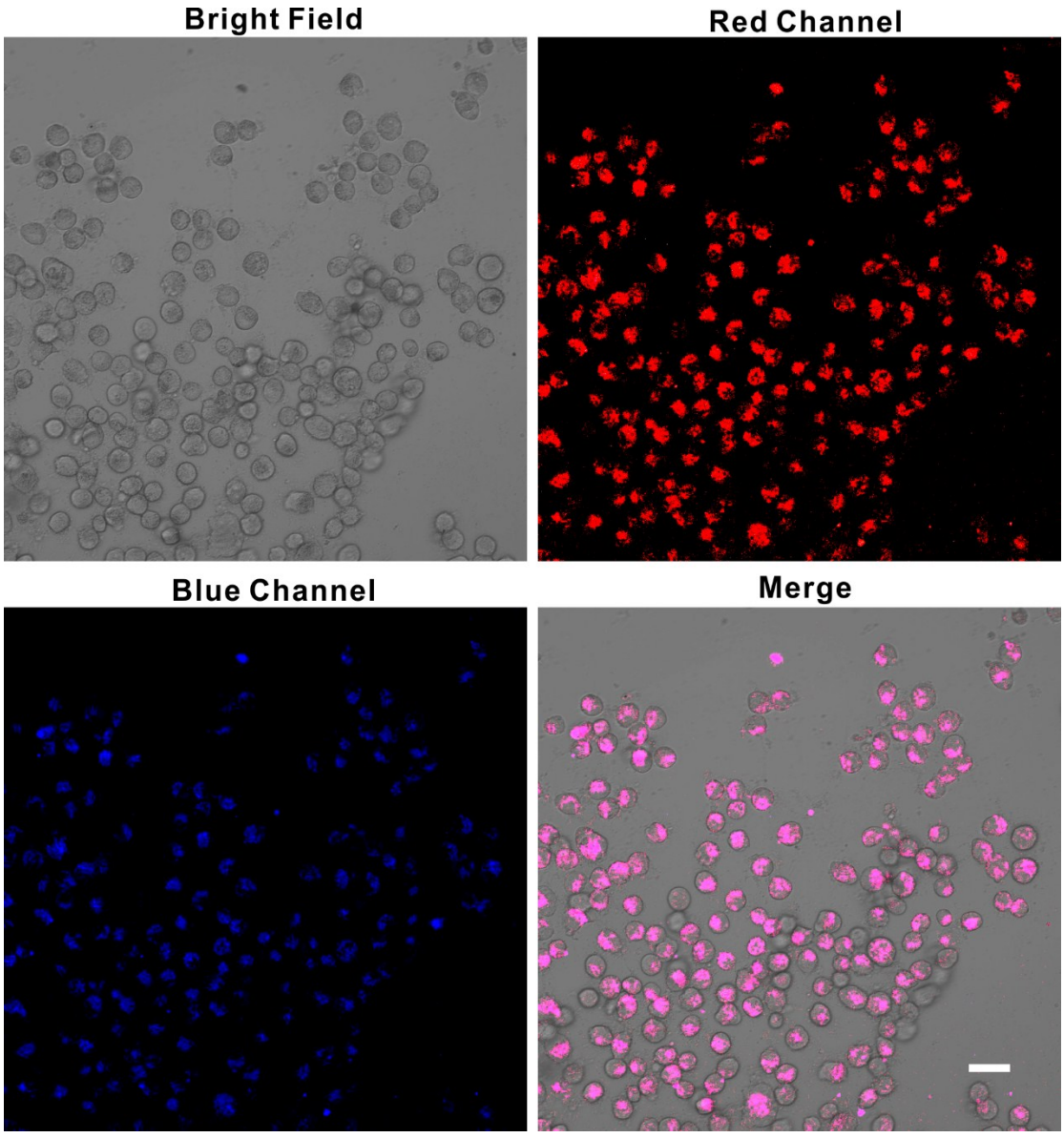

Figure S13. Enlarged bright field and fluorescence images of Hela cells incubated by d-Au NCs

and 200 μM of valine shown in Figure 4. Scar bar, 50 μm.

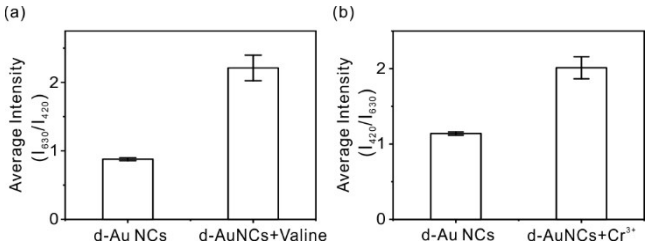

Figure S14. (a) Average fluorescence intensity analysis (I_{630}/I_{420}) for fluorescence images of d-Au NCs-incubated Hela cells with and without adding 200 μM of valine. (b) Average fluorescence intensity analysis (I_{420}/I_{630}) for fluorescence images of d-Au NCs-incubated Hela cells with and without adding 300 μM of Cr^{3+}.